Science of the Total Environment 539 (2016) 7–16

Contents lists available at ScienceDirect

Science of the Total Environment

journal homepage: www.elsevier.com/locate/scitotenv

Silver nanoparticles coated with natural polysaccharides as models to study AgNP aggregation kinetics using UV-Visible spectrophotometry upon discharge in complex environments

Pablo Lodeiro [a,b,*], Eric P. Achterberg [a,b], Joaquín Pampín [b], Alice Affatati [b], Mohammed S. El-Shahawi [c]

[a] Ocean and Earth Science, University of Southampton, National Oceanography Centre, European Way, SO14 3ZH Southampton, UK
[b] GEOMAR, Helmholtz Centre for Ocean Research, 24148 Kiel, Germany
[c] Department of Chemistry, Faculty of Science, King Abdulaziz University, P. O. Box 80203, Jeddah 21589, Saudi Arabia

HIGHLIGHTS

- UV-Visible spectrophotometry provided valuable AgNP aggregation information
- Aggregation rate of polymer-AgNPs are influenced by ionic strength and organic matter
- Fjord waters indicated strong stabilization of AgNP by natural organic matter

GRAPHICAL ABSTRACT

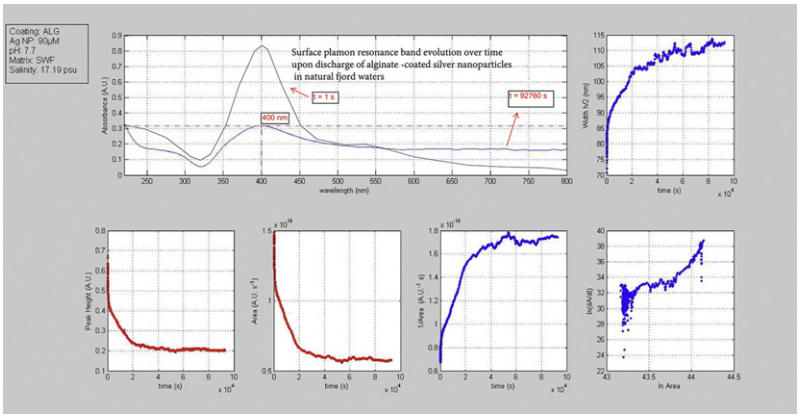

ARTICLE INFO

Article history:
Received 7 July 2015
Received in revised form 19 August 2015
Accepted 20 August 2015
Available online 9 September 2015

Editor: D. Barcelo

Keywords:
Silver nanoparticles
Aggregation
Oxidation
Alginate
Gum Arabic
Fjord waters

ABSTRACT

This study provides quantitative information on the aggregation and dissolution behaviour of silver nanoparticles (AgNPs) upon discharge in fresh and sea waters, represented here as NaCl solutions of increasing ionic strength (up to 1 M) and natural fjord waters. Natural polysaccharides, sodium alginate (ALG) and gum Arabic (GA), were used as coatings to stabilize the AgNPs and the compounds acted as models to study AgNP aggregation kinetics. The DLVO theory was used to quantitatively describe the interactions between the AgNPs. The stability of AgNPs was established using UV-Visible spectrophotometry, including unique information collected during the first seconds of the aggregaton process. Alginate coating resulted in a moderate stabilization of AgNPs in terms of critical coagulation concentration (~82 mM NaCl) and a low dissolution of <10% total Ag in NaCl solutions up to 1 M. Gum Arabic coated AgNPs were more strongly stabilized, with ~7–30% size increase up to 77 mM NaCl, but only when the silver ion content initially present in solution was low (<10% total Ag). The ALG and GA coated AgNPs showed a strongly enhanced stability in natural fjord waters (ca. 5 h required to reduce the area of the surface plasmon resonance band (SPRB) by two fold) compared with NaCl at an equivalent ionic strength (1–2 min period for a two fold SPRB reduction). This is ascribed to a stabilizing effect from dissolved organic matter present in natural fjord waters. Interestingly, for AgNP-GA solutions with 40% of total silver present as unreacted silver

* Corresponding author at: GEOMAR, Helmholtz Centre for Ocean Research, 24148 Kiel, Germany.
E-mail address: plodeiro@geomar.de (P. Lodeiro).

http://dx.doi.org/10.1016/j.scitotenv.2015.08.115

ions in the NP stock solution, fast aggregation kinetics were observed in NaCl solutions (SPRB area was reduced by ca. 50% within 40–150 min), with even more rapid removal in fjord waters, attributed to the high amount of silver-chloride charged species, that interact with the NP coating and/or organic matter and reduce the NPs stabilization.

1. Introduction

Silver nanoparticles (AgNPs) are among the most widely used NPs in consumer products, mainly because of their broad biocide activity (Chernousova and Epple, 2013; Rizzello and Pompa, 2014). Therefore, AgNPs are commonly found in medical products, textiles, deodorants, gels, cosmetics, water and air filters and household appliances (including refrigerators and washing machines) (Benn and Westerhoff, 2008; Blaser et al., 2008; Kim et al., 2007).

The increasing production of manufactured goods containing AgNPs is potentially leading to increased emissions to the environment, with possible detrimental effects on humans and ecosystems (Fabrega et al., 2011; Lapresta-Fernandez et al., 2012). While there are many uncertainties regarding emissions of AgNPs into the environment, and resulting concentrations in various compartments, there is little known about the environmental transformations (aggregation, sedimentation, oxidation, interaction with organic matter and pollutants, etc.) that determine the behaviour and fate of AgNPs upon discharge into natural waters. Factors that may control the stability and mobility of AgNPs in receiving waters include pH, ionic strength, and organic matter content, in addition to specific properties of the AgNPs, including diameter, charge, shape, concentration and coating (Auffan et al., 2010; Gondikas et al., 2012; Levard et al., 2012; Thio et al., 2011).

Once discharged into natural waters, AgNPs with weakly attached engineered or environmentally acquired coatings (not chemically bound) are often unstable and tend to aggregate. In case the coatings provide protection against dissolution, aggregation and subsequent sedimentation, then the AgNPs remain stay in solution for longer periods of time. Different capping agents (e.g. polymers and surfactants) are used to provide the NPs with required stabilities (Levard et al., 2012; Sharma et al., 2014). These compounds are added during the NP synthesis and form a coated layer on the NP surface that prevents autoaggregation through electrostatic repulsion, steric repulsion or both (electro-steric stabilization). Electrostatic repulsion provides kinetic stability while steric stabilization is usually more effective in preventing aggregation when the coating is firmly attached to the NP surface and resists degradation (Baalousha et al., 2014).

In this study, two different polyelectrolytes were used, sodium alginate (ALG) and gum Arabic (GA), to stabilize the AgNPs via electrosteric and steric phenomena, respectively. Alginates form an important component of cell walls of brown seaweed, contributing about 20–40% of the total dry weight (Percival and McDowell, 1967), and therefore this polyelectrolyte is readily found in marine waters with seaweeds. Alginic acid is a linear polymer of 1,4-linked h-D-mannuronic and α-L-guluronic acids, with pK values of 3.38 and 3.65, respectively (Haug, 1961; Rey-Castro et al., 2004). The literature regarding the manufacture and behaviour of AgNPs coated with alginate is scarce, and only one report on the synthesis of calcium-alginate-stabilized Ag and Au NPs is available (Sandip et al., 2010). There are also a few reports on the effects of alginate present in solution on the behaviour of NPs (Abe et al., 2011; Chappell et al., 2011; Gallego-Urrea et al., 2014). Even if alginate is not actually used as a coating in commercial NPs, its steric/electrostatic behaviour will act as a model for this process and its presence in the environment will potentially generate interactions with NP surfaces, so we considered it important to study its effects on AgNPs behaviour. To our knowledge, this is the first study to investigate the mechanisms of aggregation of ALG-coated AgNPs in NaCl solutions of increasing ionic strength and a natural marine water. Experiments were conducted using the ionic strength range of seawater, with chloride forming the key reactive anion with respect to silver in our experimental solutions, as is the case in natural seawater, and resulting in the formation of a range of silver chloride species (Barriada et al., 2007). We also studied the aggregation behaviour of AgNPs coated with GA, a high molecular weight polysaccharide extensively used in food and cosmetic industry (Dauqan and Abdullah, 2013). Those two industrial areas currently form important sources of AgNPs and it is therefore expected that GA is used as NP coating to improve commercial products (food packaging, soap, lipstick, etc.). Gum Arabic is a weak polyelectrolyte containing carboxyl groups (pK 2.2) (Jayme et al., 1999), which provides a strong steric stabilization to AgNPs. The effect of varying dissolved silver ion concentration on AgNP behaviour is poorly understood, and was studied here using GA-coated AgNPs with a 40% of total silver present as unreacted silver ions in the stock solution, bound to NPs and/or coating surfaces.

Therefore, we here use polymer-coated AgNPs with different physicochemical properties as models to study their aggregation kinetics in the environment. We used synthetic NaCl solutions of increasing concentrations in order to understand the aggregation mechanisms. Chloride ions occur at high concentrations in in marine waters (ca, 0.55 M at salinity 35) and form a key controlling factor in silver speciation, so their use in this work should provide us with a good approximation for the real behaviour of AgNPs in natural waters. In addition, we studied the aggregation/oxidation of polymer-coated AgNPs in natural fjord waters, in order to test their behaviour in a real marine environment, compare the results with the obtained in synthetic NaCl solutions and verify their utility as a kinetic aggregation model in more complex matrices.

The Derjaguin–Landau–Verwey–Overbeak (DLVO) theory has provided realistic descriptions of the aggregation of NPs in solution (Baalousha et al., 2013; Huynh and Chen, 2011; Li et al., 2011; Quik et al., 2014). This theory, originally applied in colloids science, describes the net energy of interactions between particles in terms of van der Waals and electric double layer interactions (Derjaguin and Landau, 1941; Verwey et al., 1948). According to the DLVO theory, upon discharge of stable NPs into the environment the balance between van der Waals attraction forces and electrostatic repulsion forces determines their stability. In solutions of increasing ionic strength the diffuse electrostatic double layer surrounding a charged NP is incrementally compressed and therefore, at high electrolyte concentrations attractive forces prevail leading to the attachment of the NPs. In contrast, at low ionic strengths when NPs are electrostatically stabilized by repulsive forces, NPs remain in solution, favouring their transport and facilitating potential ecosystem effects in natural waters. In this work we use the DLVO theory to quantitatively describe the interactions between AgNPs coated with two different polymers, simulating their discharge into the aquatic environment using NaCl solutions of increasing ionic strength (up to 1 M) and natural fjord waters.

In order to follow the aggregation kinetics of NPs in solution, we use one of the most characteristic properties of AgNPs, that is their distinctive surface plasmon resonance band (SPRB). This band is apparent at around 380–420 nm and the result of photon absorption by surface electrons on AgNPs (Amendola et al., 2010; Evanoff and Chumanov, 2005). AgNPs in solution attenuate light and consequently provide a signal in the absorption spectra (SPRB). Observations of the change in the SPRB area (A) with time by UV-Visible spectrophotometry, allows us to obtain the initial removal rates of non-aggregated AgNPs that are

proportional to the aggregation rate constants. AgNP aggregates may contribute to the SPRB signal, but these usually appear as a poorly defined band in the red region of the spectra, and can be separated from the signal of the non-aggregated NPs. Moreover, in this work we used a miniature spectrophotometer with a light source connected through optical fibres that allowed the collection of spectra in the range 250 to 800 nm in less than one second. Therefore, unique and valuable information on the first stages of the AgNP aggregation process, such as the formation of new NPs from the Ag ions, was obtained here. Moreover, the experimental setup allowed us to record full scans in a continuous manner during the entire kinetic experiment, providing valuable information of aggregation rate-stages during the process.

The aim of this work therefore is to investigate the use of AgNPs coated with natural polysaccharides as models to study AgNP aggregation kinetics upon discharge in complex environments, such as fresh, estuarine and coastal waters, represented here as NaCl solutions of increasing ionic strength (up to 1 M) and natural fjord waters.

2. Materials and methods

2.1. Synthesis of AgNPs and sample collection

AgNPs coated with gum Arabic (AgNP-GAL and AgNP-GAH, where L denotes low Ag^+ and H high Ag^+ content) and alginate (AgNP-ALG) were synthesized by chemical reduction of a silver nitrate salt following the established methods (Lin et al., 2012; Ma et al., 2012), with minor modifications. The total silver concentration (Ag^+, Ag^+-complexes and Ag^0) in the original solution batches as determined by ICP-MS (Quadrupole Thermo X-Series 2) of AgNP-GAL was 195 ± 9.3 μM with around 0.2% of the total silver as Ag^+ in solution, and for the AgNP-GAH was 98.3 ± 3.1 μM with around 37% of the total silver as Ag^+ bound to AgNPs and/or coating surfaces. The total silver concentrations of the original batch solutions of AgNP-ALG and ^{109}AgNP-ALG (silver stable isotope 109 is usually used as tracer; Ag107 is naturally occurring isotope) were 668 ± 43 μM (0.2% of total silver as Ag^+ in solution) and 556 ± 4.7 μM (0.03% of total silver as Ag^+ in solution), respectively. These silver isotopes were used here due to their slightly different characteristics (Table 1) in terms of width of the SPRB at half height ($W_{h/2}$) and ζ-potential (ζ). These concentrated stock solutions were diluted and used in the experiments. Details of AgNPs synthesis can be found in the supplementary information (SI).

The chemicals used throughout the experiments were purchased from Sigma-Aldrich (Dorset, UK) and Fisher Scientific (Leicestershire, UK). High-purity water (MilliQ, Millipore, Watford, UK) with a resistivity of 18.2 MΩ cm was used.

The natural fjord water surface sample was collected in Kiel fjord (54.368° N, 10.195° E), located in northwest Germany, and stored in an acid-cleaned low density polyethylene (LDPE) bottle (Nalgene) until use. A complete sample characterization can be found in the SI.

Table 1
Variables measured to establish the stability of the manufactured AgNP stock solutions over time: pH, surface plasmon resonance band (SPRB), width of the SPRB at half height ($W_{h/2}$), ζ-potential (ζ), hydrodynamic diameter (d_h), diameter (TEM), total silver (Ag_{total}) and free silver ions and its complexes (Ag^+). The standard deviations of at least two different measurements are shown between parentheses.

	AgNP-ALG	^{109}AgNP-ALG	AgNP-GAL	AgNP-GAH
pH	5.8–6.2	5.6–6.2	5.5–6.1	5.4–6.3
$SPRB_{max}$ (nm)	398–399	394–396	398–400	398–401
$W_{h/2}$ (nm)	65.5–64.8	56.5	63.0	56.8–57.5
ζ (mV)	−70 (6.7)	−48 (8.9)	−41 (7.1)	−43 (6.3)
d_h (nm)	33 (3.3)	35 (3.9)	55 (6.0)	–
Diameter (nm)	9.7 (0.44)	–	10 (0.29)	–
Ag_{total} (μM)	668 (43)	556 (4.7)	195 (9.3)	98.3 (3.1)
Ag^+ (%)	0.2–2	0.03–3	0.2–8	37–44

2.2. Experimental techniques and equipment

The AgNPs batches used in the experiments were periodically characterized through measurement of pH and silver ion content in solution, and determination of the position, area (*A*) and $W_{h/2}$ in a UV-Visible spectrum (Fig. S1). Other techniques such as transmission electron microscopy (TEM) and Flow-field flow fractionation (F-FFF) were also used to determine AgNP size (Figs. S2–S3 and more details in the SI).

- UV-Visible spectrophotometry.
  The UV-Visible spectra were recorded using a deuterium tungsten halogen light source (DT-Mini 2GS, Ocean Optics), a quartz cuvette and a miniature CCD array spectrophotometer (USB-4000, Ocean Optics), connected through two optical fibres (600 μm fibre, P600-025-SR). Using this set-up we were able to obtain a complete scan (from 250 to 800 nm) in <1 s. A control solution without AgNPs was used to blank correct the instrument before the start of the measurements. The solutions at fixed pH (8.0 ± 0.2), with a range of AgNP, total silver concentrations (44 and 90 μM), different NaCl concentrations (from 0 to 997 mM) and also natural fjord waters, were analysed in terms of SPRB evolution (*A*, $W_{h/2}$, SPRB height and position of the absorbance maximum) over time (Videos S1–S8). The same integration time (100 ms), number of averaged scans (3) and boxcar smoothing (10) were used during the experiments. At least two replicates were measured for each experiment. In order to avoid possible contributions to *A* of AgNP aggregates, that would present absorption at higher wavelengths (>500 nm), we obtained *A*, $W_{h/2}$, SPRB height and position of the absorbance maximum from a straight line traced from the base of the SPRB between 325 and 500 nm. An in-house Matlab script was used to record a full spectrum (from 250 to 800 nm) every second at the beginning of the aggregation process when the changes of the SPRB were fast, and increasing this time step as the experiment proceeded. The experiments were conducted until the SPRB disappeared in the case of fast aggregation processes, and for at least 1500 s in the case of slow processes.
- Inductively Coupled Plasma Mass Spectrometry (ICP-MS).
  Silver content was measured by ICP-MS after dilution and digestion of the samples with 0.3 M HNO_3 (70%; Optima, Fisher Scientific). Oxidation experiments were undertaken to verify the AgNP stability in terms of solubilisation in the original batches and during the experiments. Silver ion (Ag^+) concentrations in solution produced during the dissolution of the AgNPs were determined using different approaches depending on the sample matrix. At negligible Cl^- concentrations an Ag Ion Selective Electrode (Ag-ISE) from Thermo Scientific (9616BNWP) was used. For saline matrices, separation of Ag^+ (free silver ion and its complexes) and AgNP was necessary. We carried out the separation by ultrafiltration using centrifugal ultrafilters (3 kDa, Amicon Millipore) and a centrifuge (5430R, Eppendorf). Subsequent quantification of Ag^+ and total silver in the filtrate and retentate was carried out by ICP-MS.

2.3. Aggregation kinetics of AgNPs: model background

The evolution of the AgNPs absorption spectra with time provided data to determine the aggregation kinetics of NPs. Therefore, the reduction in *A* was monitored in order to follow the aggregation kinetics at different NaCl concentrations and in natural fjord waters. The critical coagulation concentrations (CCCs), were calculated when possible, as they provide a simple stability limit of a NP suspension. The SPRB is due to excitation of the conduction electrons in the particles. The changes in the SPRB area reflect an overall aggregation process of the AgNPs present in solutions. This probably includes not only non-aggregated AgNPs, but also small clusters. The calculations were done measuring the decrease of the SPRB area at the beginning of the aggregation

process, when aggregate formation commenced. We did not observe significant changes in the position of the SPRB maximum or appearance of secondary peaks during that time window. The SPRBs depend on AgNP size, shape, dielectric constant of the medium, and electromagnetic interactions among adjacent particles. Isolated silver spheres have only one plasmonic resonance due to their symmetry, but new resonances can appear when they are organized in small assemblies. Therefore, multimers have new resonance modes with a higher absorption wavelength that the shown by isolated AgNPs (Amendola et al., 2010). Therefore, we consider that non-aggregated AgNPs are the only entities contributing to the size of the area under the SPRB. Consequently, the reduction in the SPRB value, due to the decrease in the number of surface electrons in the NPs, can be related to the change in Ag nanoparticle concentration containing an average number of silver atoms, and can be described by the following reaction law (Espinoza et al., 2012):

$$\text{SPRB area rate change} = \frac{dAg_a}{dt} = \frac{dA}{dt} = -kA^n \quad (1)$$

where Ag_a is the concentration of silver atoms in the solution (M), A is the area under the SPRB (A.U. s^{-1}), k (s^{-1}) the aggregation rate constant and n the reaction order. Two different mechanisms can dominate the AgNP removal kinetics in the presence of NaCl: oxidative decomposition, at [NaCl] < 25 mM, and aggregation, at higher NaCl concentrations (Espinoza et al., 2012). Oxidative decomposition is a relatively slow process due to the passivation of the AgNP surface by silver chloride species and/or other by-products formed during the reaction. When oxidation is the dominant mechanism, a representation of ln (dA/dt) vs ln (A) should provide a straight line with a slope, n, of around 0.67. The AgNP dissolution is here proportional to the NP surface area per unit volume of solution (Espinoza et al., 2012).

In contrast, if aggregation dominates, the decrease in A can be ascribed to AgNP removal due to attachment of two non-aggregated NPs, providing a reaction rate of the order two. Therefore, integrating Eq. (1) for n = 2 the following is obtained:

$$\frac{1}{A} = \frac{1}{A_0} - kt. \quad (2)$$

A plot of the inverse of A vs t should then provide a straight line.

ALG and GA-coated AgNPs presented a negative surface charge in the experimental solutions (Table 1). The presence of these electrostatic charges in solution affects the interaction between NPs and the surrounding medium. Therefore, electrostatic considerations should be taken into account in the modelling efforts. Speciation calculations using the software MINTEQ+ were conducted for the fraction of silver that was not reduced during the manufactured procedure (Fig. S4). These indicated that the saturation index of AgCl (mineral cerargyrite) is not achieved even at high NaCl concentrations (600 mM). The main soluble silver species formed in presence of NaCl at pH of 8.0 are $AgCl_{aq}$, $AgCl_2^-$, $AgCl_3^{-2}$ and $AgCl_4^{-3}$, in agreement with other studies (Barriada et al., 2007). Only at NaCl concentrations lower than 20 mM, is the neutral compound $AgCl_{aq}$ the dominant species together with $AgCl_2^-$. As the NaCl concentration is increased, $AgCl_2^-$ represents the principal silver compound up to 200 mM, from where $AgCl_4^{-3}$ and $AgCl_3^{-2}$ contribute with more than 20% to the total species present in solution (Fig. S4).

The interactions between suspended AgNPs as a result of Brownian motion can be described according to DLVO energy profiles. DLVO theory assumes that the interaction free energy per unit area between two particles can be estimated by two additive contributions, namely van der Waals and double layer interactions. In this study, NPs with a charged surface are studied and repulsive electrostatic double layer interactions could dominate their stability, especially at lower salt concentrations. In contrast, at high salt concentrations and/or low surface charge, the interactions between NPs are dominated by the attractive van der Waals forces.

We assume that aggregation starts with a dimer formation from two non-aggregated NPs, based on the Smoluchowski principle (Chandrasekhar, 1943), and that aggregates of any size will form with an identical kinetic rate constant k; subsequently aggregated-NPs and/or aggregate-aggregate interactions can occur forming unstable suspensions. The aggregation rate constant is proportional to the slope of the change on A over time during the early stages of the aggregation, when formation of dimers is considered important, according to Eq. (2).

At enhanced ionic strengths the electrical double layer surrounding the NPs is compressed, and the role of electrostatic interactions in the aggregation process is screened. Van der Waals forces and hydrodynamic interactions are minor and the aggregation kinetic is controlled by Brownian diffusion. This regime is known as fast aggregation or diffusion controlled aggregation (DCA). In contrast, at lower ionic strengths double layer interactions between the charged NPs result in an energy barrier. As a consequence, the aggregation rate is reduced and the NPs remain in solution for longer. This regime is known as slow aggregation or reaction controlled aggregation (RCA), due to mechanistic similarities to chemical reactions.

Normalizing the slopes obtained at different salt concentrations to the one obtained in the DCA regime, under favourable aggregation conditions, the aggregation efficiency (α), which represents the fraction of successful aggregation, can be calculated by:

$$\alpha = \frac{k}{k_{DCA}} = \frac{\left(\frac{dA}{dt}\right)}{\left(\frac{dA}{dt}\right)_{DCA}}. \quad (3)$$

Plotting the evolution of α against the NaCl concentration, the CCCs can be obtained as the intercept between the RCA and DCA regimes. When the NaCl concentration exceeds the CCC at α of 1, the NPs double layer is sufficient suppressed to allow NPs to approach each other, resulting in rapid aggregation. As a consequence, above the CCC when NPs double layer is suppressed, DCA occurs with the rate of change of A almost independent of the electrolyte concentration.

The SPRB evolution was followed from the first second after the AgNP addition to the solutions containing various NaCl concentrations and natural fjord waters. To our best knowledge this is the first time that UV-visible spectral data for AgNP were obtained from the initial stages of a NP aggregation process, which helps to understand and quantify the AgNP interactions during early stages of aggregation. The CCC values are obtained using UV-Visible spectrophotometry by determining A or $W_{h/2}$ evolution over time at different NaCl concentrations (from 0 to 997 mM). The $W_{h/2}$ is related to the SPRB height and also to its area. Therefore, it is expected that this parameter may also be useful to calculate parameters such as the CCC, as demonstrated in the manuscript. Moreover, A also allows us to assess the dominant mechanism of AgNP removal, through oxidation and/or aggregation.

3. Results and discussion

3.1. AgNPs characterization

In order to verify the stability of the synthesized AgNPs over time, the following variables were frequently measured in the stock solutions: pH, Ag_{total} and Ag^+ concentrations, $W_{h/2}$, position of the SPRB, ζ-potential, hydrodynamic diameter (d_h), and NP diameter using TEM. The obtained values for AgNP-ALG, ^{109}AgNP-ALG, AgNP-GAL and AgNP-GAH are presented in Table 1. A detailed explanation of the AgNP characterization can be found in the SI.

3.2. AgNPs aggregation and dissolution kinetics

The SPRB area evolution over time was followed by UV-Visible spectrophotometry in solutions containing a fixed initial amount of AgNPs (44 or 90 μM). Upon addition of NaCl to the solution, the pH was

adjusted to 8.0 ± 0.2. In absence of NaCl, AgNPs were stable over time in terms of aggregation (Fig. S1). With increasing NaCl concentrations, different behaviours were observed depending on the type of polymer used as coating for the AgNPs. Natural fjord water was also used in the kinetic aggregation experiments.

3.2.1. AgNP coated with alginate

AgNP-ALG and ^{109}AgNP-ALG behaved according to the DLVO aggregation theory. Fig. 1 shows the characteristic fast and slow aggregation kinetic regimes obtained by UV-Visible spectrophotometry.

At pH 8 the main acid groups present in alginate (−COOH) are deprotonated (Rey-Castro et al., 2004) providing the AgNP with a net negative charge (see ζ-potential values in Table 1). In this case, the alginate coating stabilizes the AgNP suspension by electro-steric repulsion, and consequently in low ionic strength solutions aggregation is prevented. Nevertheless, at enhanced NaCl concentrations a plot of $1/A$ vs t (Eq. (2)) yielded straight lines with high regression coefficients, confirming the aggregation process (Video S2).

The area under the SPRB curve in the frequency spectrum is proportional to the quantity of surface electrons in the AgNPs and consequently to the concentration of silver atoms in the solution (each silver atom donates one electron to the metal). Therefore, the increase in peak area confirmed the formation of new small NPs from Ag^+ reduction in the presence of low amounts of Cl^- ions and/or silver-chloride species. The SPRB evolution over time at different NaCl concentrations is shown in Videos S1–S2. For NaCl concentrations ≤ 42 mM there was an increase in A between 5–25 s and finally a constant value was achieved (inset Fig. 1a). Small varying trends were also observed at longer times for the lowest salt concentrations tested. Nevertheless, at [NaCl] > 61 mM a rather continuous reduction of A was observed (Figs. 1b, S5a–b).

The percentage increase in A that occurred during the first 25 s is presented in Table S2. At NaCl concentrations higher than 58 mM for AgNP-ALG and 50 mM for ^{109}AgNP-ALG, there was no observable increase in A, so contributions from the formation of new AgNPs from the silver ions are not expected. Usually, the time required for the collection of a full spectrum using a standard bench-top laboratory spectrophotometer is ≥25 s, and therefore important information, such as the possible formation of new NPs from the silver ions present in solution, is missed. In this study, we obtained a full spectrum from the first second of a NP aggregation process, which facilitated our interpretation of AgNP behaviour at the early stages of aggregation.

The CCC values obtained for AgNP-ALG and ^{109}AgNP-ALG, following the evolution of A in the RCA and DCA regimes, were 80 ± 9.3 and 82 ± 4.2 mM (Fig. 2).

The relatively high error in these values was associated with the uncertainty in the selection of the time window for the initial aggregation stage, where the NP dimers are formed. Different linear steps following Eq. (2) were observed in the aggregation process depending on the NaCl concentration. Two or three regions with different slopes of change of A with time were noted as the aggregation proceeded, corresponding to different aggregation rates (Fig. 1 and Video S2).

CCC represents the minimum NaCl concentration required to destabilize the NPs in solution, providing an important indicator for AgNPs stability. The obtained values using different polymer-coated AgNP can be used to predict their behaviour and fate in natural systems at specific ionic strengths and in the absence of organic matter.

The $W_{h/2}$ evolution was determined over time in order to track possible changes to the AgNPs surface, including adsorption–desorption of different species and oxidation layer formation (Fig. S6a–b and Videos S1–S2). The $W_{h/2}$ values obtained at [NaCl] = 31 mM showed a decrease relative to those observed in the absence of NaCl. The SPRB

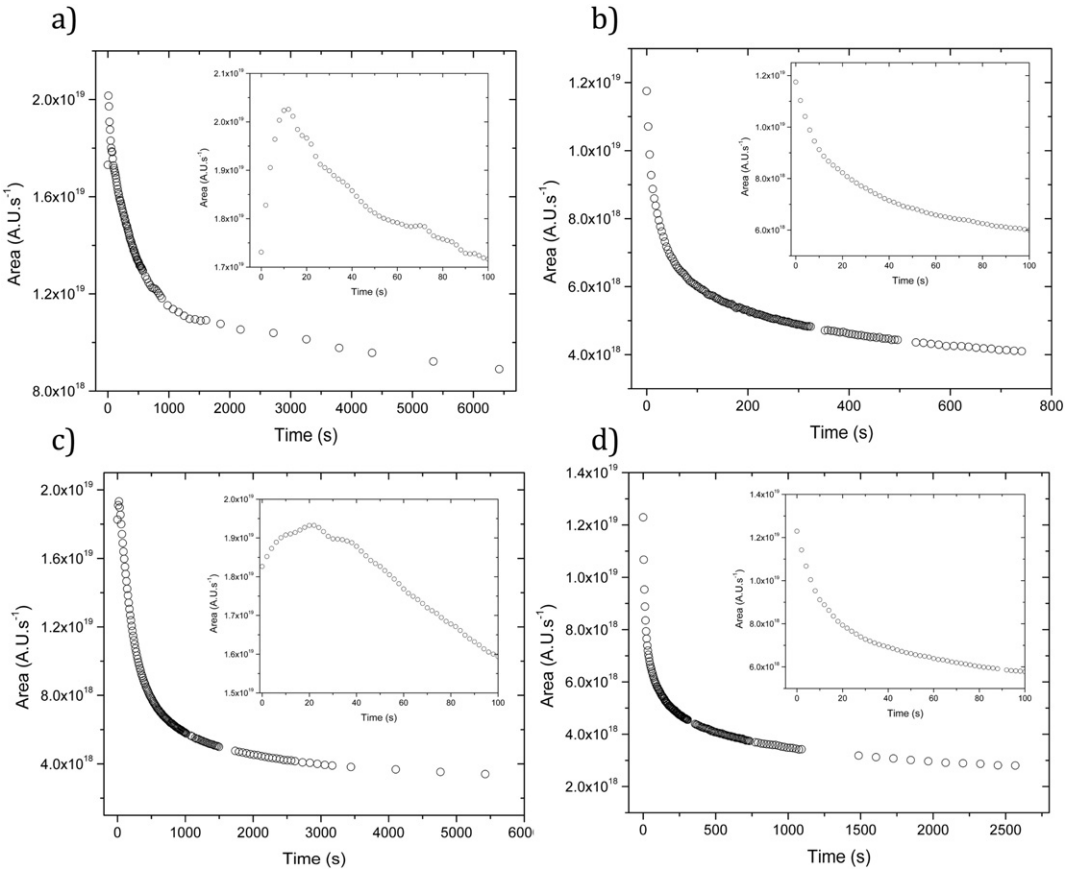

Fig. 1. SPRB area, A, evolution over time for AgNP-ALG in NaCl 42 mM (a) and 153 mM (b), and for ^{109}AgNP-ALG in NaCl 42 mM (c) and 153 mM (d). The insets represent enlarged regions for *the first 100 s*.

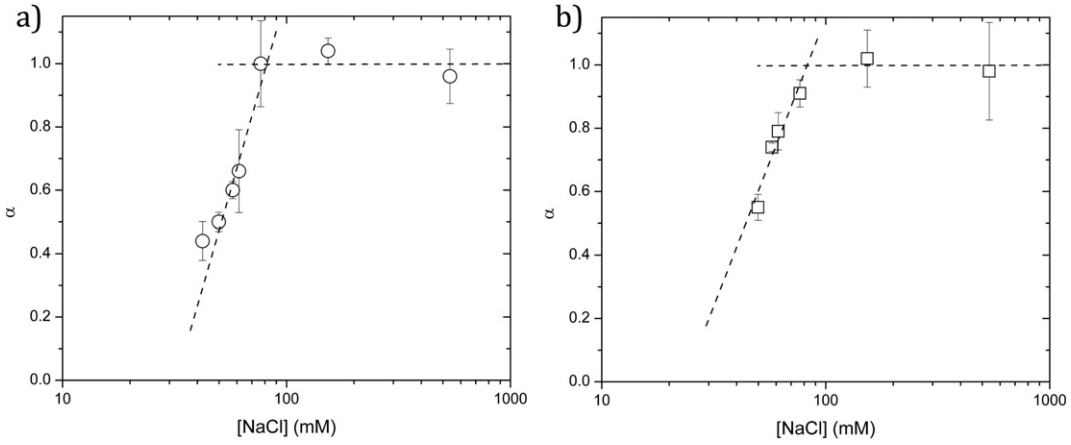

Fig. 2. Aggregation efficiencies obtained from the changes over time of A using a) AgNP-ALG and b) ^{109}AgNP-ALG at different NaCl concentration. Error bars represent the standard deviation of at least two replicates of the same experiment.

narrowing in presence of NaCl indicated that the surface species (possibly ALG coating or Ag species) are being replaced by chloride ions (Espinoza et al., 2012). Nevertheless, at [NaCl] > 31 mM, $W_{h/2}$ increased with time (up to 180 nm) until a constant value was reached at the end of the experiment. At enhanced NaCl concentrations, the AgNP aggregation could contribute to the widening of the SPRB due to light absorption of the aggregates and/or non-spherical nanoparticle shapes at wavelengths higher than 500–550 nm.

Moreover, the slopes observed for the $W_{h/2}$ evolution at the beginning of the process, increased with NaCl concentration up to 77 mM. At higher salt concentrations the slopes were rather similar, and identical to what was observed by plotting the evolution of α against NaCl concentration (Fig. 2). Therefore, the $W_{h/2}$ evolution over time also provided a good approximation for CCC values.

The AgNPs oxidation experiments indicated that the presence of Ag^+ species in solution increased from 2 to 9% of the total silver content within 20 min at 537 mM NaCl. Therefore, it is possible that AgNP dissolution also played a role in aggregation kinetics. The AgNP oxidation could not be confirmed by a plot of ln (dA/dt) vs ln (A) and verification of the obtained slopes, as these were different (values between 3.6 and 6.8) to the theoretical value (0.67) expected for oxidation processes (see SI, Videos S1 and S2).

The analysis of the AgNP-ALG aggregation in the natural fjord waters is presented in Figure S7a–b and Video S3, where the evolution of the SPRB with time is presented.

The fjord water sample had a pH of 7.7 and a salinity of 17.19, which is equivalent to a chloride concentration of ca. 270 mM. This salt concentration is higher than the CCC value found in NaCl (~81 mM), so a rapid aggregation kinetic of alginate-coated AgNP is expected upon discharge into the fjord waters. However, comparison of the *A* decrease during the first stage of aggregation in a NaCl solution ([NaCl] ≥ 153 mM) and in natural fjord waters, shows a much slower aggregation rate for the natural water (Fig. 3).

During the time window (~40 s) over which the CCC values were calculated, a 38% decrease in *A* for NPs in NaCl solutions (153 and 537 mM) was observed, while for identical ALG-coated NPs deposited in natural fjord waters, *A* remained stable (^{109}AgNP-ALG) or showed a minor reduction of 10 ± 0.35% (AgNP-ALG). Moreover, if the time required to decrease *A* by half is compared, we observed significant differences between the artificial and natural waters. A period of 1–2 min was sufficient to decrease the initial value of *A* in NaCl solutions (153 and 537 mM) by two fold (Fig. 3); nevertheless, for natural fjord waters a period of ca. 5 h was required to obtain an identical reduction in *A* for the ALG-coated NPs (Video S3).

These observations highlight the influence of the complex environment in the fjord waters compared to the synthetic NaCl solution. A detailed analysis of the natural fjord water sample is shown in Table S3. The total organic carbon content was high (277 μM) compare to the values usually found in seawaters (<80 μM). Fluorescence dissolved organic matter (FDOM) and chromophoric dissolved organic matter (CDOM) analyses confirm the presence of different types of organic compounds in solution. The position of the emission and excitation bands shown in FDOM measurements (Fig. S8a) corresponded to fluorescent species from different sources: terrestrial humic-like (A-peak)

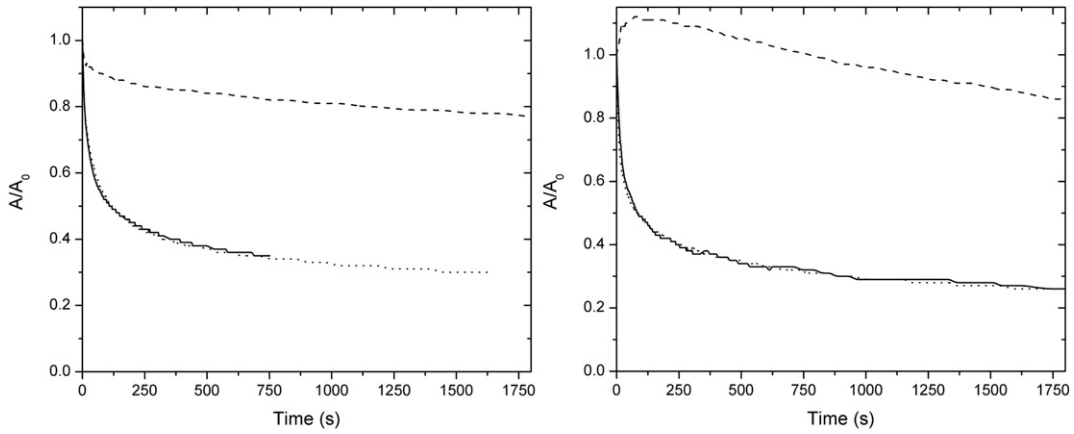

Fig. 3. Normalized SPRB area (A/A_0) evolution over time for AgNP-ALG (left) and ^{109}AgNP-ALG (right) in natural fjord waters (dashed lines), 153 mM NaCl (solid lines) and 537 mM NaCl (dotted lines).

and terrestrial fulvic-like (C-peak), in agreement with other reports for fjord waters (Coble, 2007; Ishii and Boyer, 2012). CDOM from fjord waters represents a complex pool of substances rich in humic/fulvic materials that originate from terrestrial sources. A CDOM absorption coefficient, a_{355}, of 2.55 m^{-1} was obtained at 355 nm. Absorption is a proxy for the concentration, while the spectral slope, S = 0.010 nm^{-1} (between 280 and 312 nm), describes the steepness of the spectrum and is used to account differences in CDOM composition (Fig. S8b). Both measurements, CDOM and FDOM, showed high terrestrially derived organic matter inputs (Sulzberger and Durisch-Kaiser, 2009).

No significant differences were found in the aggregation/oxidation behaviour of the stable, 109-Ag, and naturally occurred, 107-Ag, isotopes, despite their slightly different $W_{h/2}$ and ζ-potential.

3.2.2. AgNP coated with gum Arabic: AgNP-GAL

In contrast to AgNP-ALG, the exposure of AgNP-GAL to increasing NaCl concentrations had only a minor effect on their aggregation process for periods up to 25 min. Moreover, there was no clear correlation between the aggregation rate constant (k) and the NaCl concentration, as is expected for a system following the DLVO colloid theory.

At NaCl concentrations < 153 mM and experimental durations lower than 1500 s, the A values showed very small changes (Fig. 4 and Video S4). For [NaCl] ≥ 153 mM over the same time window, the A decreased with time to values between 3 and 41% of its initial value. Moreover, at the highest NaCl concentrations tested (537 and 997 mM) a linear decrease of around 75–80% of the initial A was observed after 3–4 h (Video S5).

High correlation coefficients were obtained through fitting Eq. (2) to UV-Visible data, (Video S5), demonstrating that aggregation of NPs is contributing to the decrease in A, but slower than for AgNP coated with alginate.

As ζ-potential measurements indicate (Table 1), the NPs were negatively charged. Even if a CCC value could not be obtained, some electrostatic stabilization contribution is expected as indicated by the minor tendency to aggregate (Fig. 4). However, the increase in ionic strength alone does not explain the aggregation kinetic behaviour. GA is polymer with a high molecular weight (5×10^4 to 8×10^6 g/mol), with a strong steric stabilization power (Jayme et al., 1999; Lin et al., 2012). The behaviour of AgNP-GAL is hence not entirely dependent on the electrostatic forces, and therefore it appears that the GA coating stabilizes the NPs predominantly due to steric effects. Nevertheless, the steric stability provided by the GA coating disappeared at long experimental times and enhanced NaCl concentrations.

In order to investigate the changes observed in the steric stability of AgNP-GAL, the $W_{h/2}$ evolution was determined over time (Fig. S6c). At [NaCl] < 153 mM, the $W_{h/2}$ values were lower than those observed in the absence of salt. Moreover, a decrease over time was observed for [NaCl] < 60 mM during the first 10 s of the experiment. This SPRB narrowing could indicate that surface species are replaced by chloride ions and consequently prevent NP aggregation. In contrast, at highest NaCl concentrations (537 and 997 mM), increases in $W_{h/2}$ were observed, which was clearly related to the formation of AgNP aggregates contributing to the increase in absorbance at high wavelengths and modifying the shape of the SPRB. As observed for AgNP-ALG, a wide and poorly defined band appeared at wavelengths between 500 and 750 nm for the highest NaCl concentrations (Video S5). This band was also observed by other authors (Baalousha et al., 2013; Moskovits and Vlčková, 2005).

Moreover, no evidence for new AgNP formation from silver ions was observed by UV-Visible spectrophotometry (Table S2).

The AgNP-GAL dissolution experiment indicated that the presence of Ag^+ species in solution increased from 8.5 to 9.5% of the total silver content for NaCl concentrations of 0 and 537 mM. Therefore, AgNP oxidation under the conditions tested was of minor importance. A plot of ln (dA/dt) vs ln (A) produced slopes with values between 1.4 and 2.6, different to the theoretical value expected for an oxidation process (0.67).

On the other hand, as was observed for ALG-coated NPs, the addition of AgNP-GAL to natural fjord waters produced a noticeable additional stabilization against aggregation of the NPs compared to NaCl solutions at equivalent chloride concentration (Fig. 5).

More than 15 h after the introduction of AgNP-GAL to the fjord waters, no appreciable aggregation was observed with only 2% decrease in A (Video S6). Nevertheless, within only 25 min the SPRB area decreased 12 ± 1.5% when AgNP-GAL was added to NaCl (153, 537 mM), with a two fold decrease in A after 1 h. This indicates the important role of natural organic matter presented in the fjord waters on the stabilization of the AgNP-GAL, reducing aggregation in solution at a salinity of 17.19 due to steric-electrostatic forces (Fig. S7c). Therefore, it is crucial to elucidate the role of organic matter in natural waters, in order to better understand behaviour and fate of discharged NPs.

3.2.3. AgNP coated with gum Arabic: AgNP-GAH

Inefficient purification during the manufacturing of AgNPs will lead to the presence of unreacted silver ions in the NP stock solution. Unreacted silver ions may also occur in solutions due to AgNP dissolution. The high affinity of the non-reduced silver ions for the NP coating and/or surfaces is expected to influence AgNPs behaviour in terms of aggregation and oxidation. This phenomenon is poorly understood and was studied here using GA-coated AgNPs. The steric stabilization of GA coating was not noticeable in case the AgNP-GA solutions contained enhanced concentrations of Ag^+ (AgNP-GAH with >40% of the total silver content as soluble Ag^+ bound to the NPs and/or coating surfaces). This was likely due to changes in the coating layer structure and/or adsorption due to interactions with different silver-chloride species present in excess and interacting with the AgNPs.

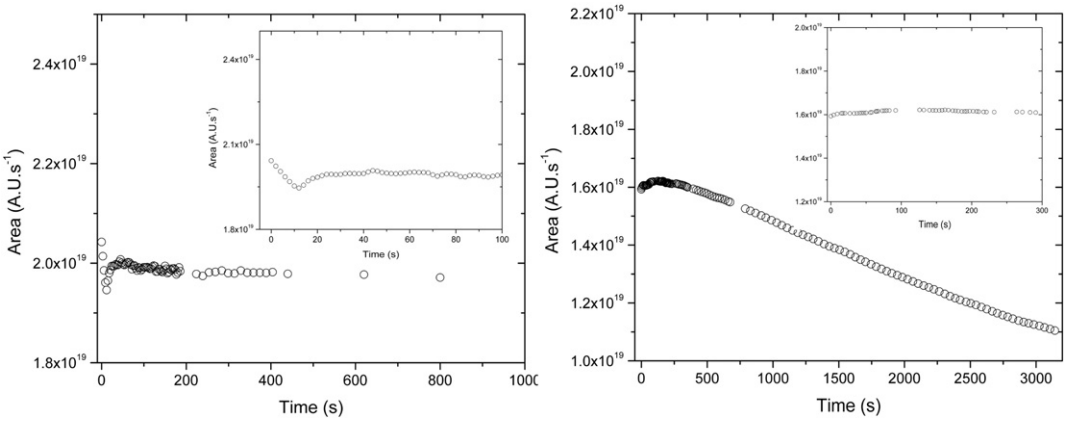

Fig. 4. SPRB area evolution over time for AgNP-GAL at different NaCl concentrations: 50 (left) and 153 mM (right). The insets represent an enlarged region for the first 100 s.

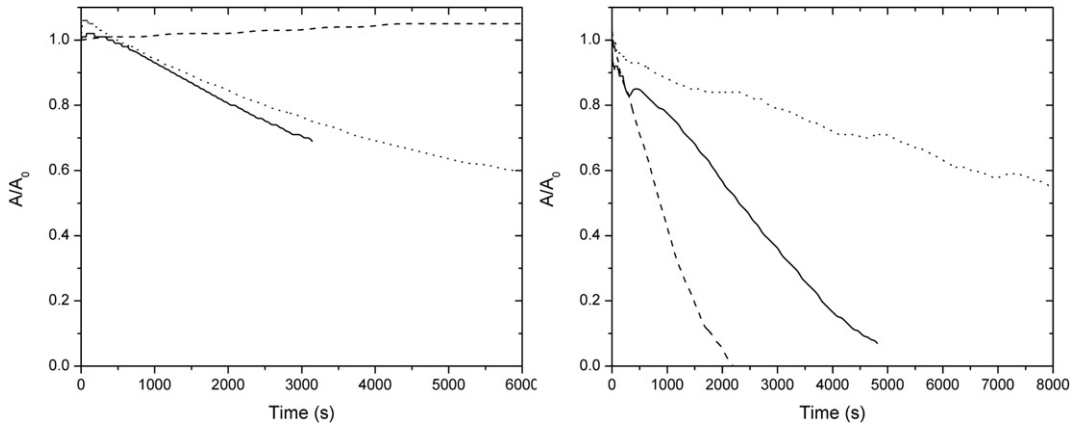

Fig. 5. Normalized SPRB area, A/A_0, evolution over time for AgNP-GAL (left) and AgNP-GAH (right) in natural fjord waters (dashed lines), 153 mM NaCl (solid lines) and 537 mM NaCl (dotted lines).

The reduction in *A* (Fig. 6) was determined and yielded a CCC of 45 ± 0.73 (Fig. 7) (not considering [NaCl] > 77 mM).

Two different types of behaviour were observed depending on NaCl concentration. At [NaCl] < 153 mM the SPRB evolution experiments indicated strong variations in area together with more constant stages, and finally after 200–600 s a linear decrease was observed until the SPRB disappeared in 50–80 min (Fig. 6, Video S7). At higher salt concentrations a different behaviour of the SPRB was observed. In the first 65 s *A* showed strong variations, but subsequently it decreased more slowly, at enhanced salt concentrations, until it disappeared in linear manner after more than 1.5–5 h for 153 and 537 mM NaCl, respectively (Fig. 6, Video S8).

The slopes and regression coefficients for the linear regression fit of *A* reduction (Eq. (2)) confirmed that aggregation was the main mechanism involved at NaCl concentrations up to 77 mM. The unexpected behaviour observed at higher NaCl concentrations, which presented a slower aggregation kinetic, was attributed to the high amount of silver species ($AgCl_2^-$, $AgCl_3^{-2}$ and $AgCl_4^{-3}$) immediately surrounding the NPs that could act as a protection layer for the NP surface, delaying the aggregation phenomena. Moreover, a steric stabilization contribution could also be possible due to conformational changes in the GA coating structure that may occur at very high NaCl concentrations in presence of unreacted silver ions from the NP stock solution.

Figure S6d shows the $W_{h/2}$ evolution over time for AgNP-GAH. In contrast to ALG-coated NPs, a rather continuous decrease of $W_{h/2}$ was observed for [NaCl] ≤ 153 mM. This narrowing of SPRBs was associated with the substitution on the NP surface of AgO_2 and/or GA with silver chloride species formed as a consequence of the high initial concentration of silver ions present in the NP stock solution. Therefore, the SPRB narrowing was more noticeable than in the AgNP experiments. The slopes of $W_{h/2}$ vs *t* were similar for salt concentrations between 42 and 153 mM, and as a consequence a CCC value of ca. 42 mM is obtained, in agreement with the value derived from the *A* evolution over time. In contrast, at the highest NaCl (537 mM), $W_{h/2}$ values were greater than the value obtained in absence of salt and also stable over time. That behaviour reflects the influence of silver species initially present in the AgNP stock solution on the aggregation kinetic, at NaCl concentrations equivalent to those in marine waters. Therefore, thorough NP purification is required as part of the manufacturing process with a detailed NP characterization including silver ions analysis in the stock solution. It is well established that silver ions are highly toxic and persistent in ecosystems. However, it is still unclear to which extent the toxic effects of AgNPs arise from their capacity to release of silver ions or from specific characteristics of NPs themselves, or both. In this work we show how the presence of silver ions, due to incomplete reduction during AgNP manufacturing, greatly influence the aggregation/oxidation behaviour of the AgNPs. The concentration of silver ions present in AgNP aggregation studies is usually very low, and therefore their effect is limited. In this work we studied the influence of silver ions at a concentration equivalent to the 40% of the total silver concentration in solution. We consider this fact relevant since little is know about the influence of the environmental effects of silver ions, released after AgNPs oxidation, or present when they are discharged together with AgNP in solution.

New AgNP formation from ions occurred during the first 5–25 s of NaCl–AgNP interaction for [NaCl] ≤ 153 mM (Table S2).

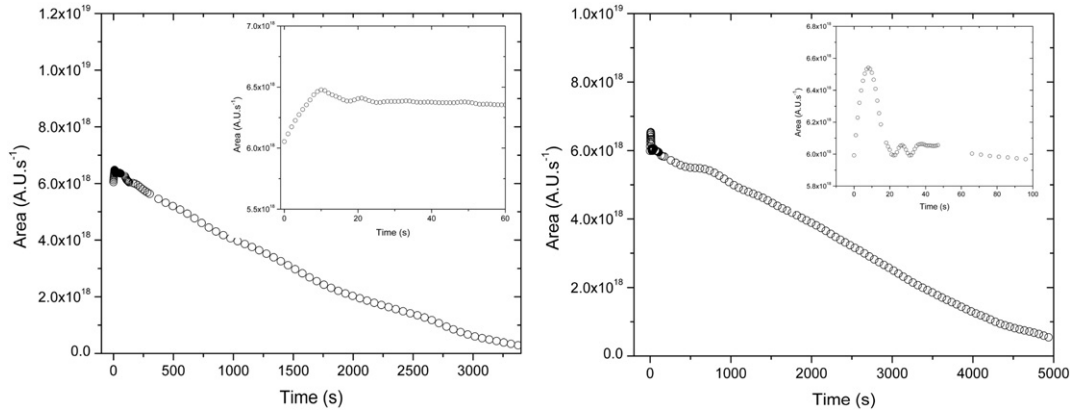

Fig. 6. SPRB area evolution over time for AgNP-GAH at different NaCl concentrations: 42 (left) and 153 mM (right). The insets represent a zoom region for the first 100 s.

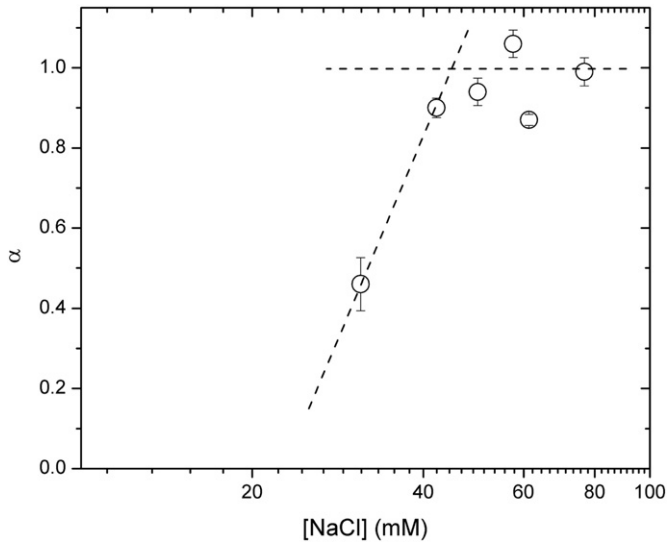

Fig. 7. Aggregation efficiencies obtained from the changes over time of A of AgNP-GAH at different NaCl concentration. Error bars represent the standard deviation of at least two replicates of the same experiment.

Dissolution experiments with AgNP-GAH showed that the concentration of Ag^+ (silver chloride species) in solution increased after 200 min from 44 to 65 ± 5%, independent of the NaCl concentration (31 or 537 mM). Therefore, after more than 3 h only 35% of the total silver was in the form of AgNP (not considering aggregation). The oxidation of the AgNPs was monitored during the aggregation kinetic studies, but was only detected after the SPRB disappearance. This fact implies that there were not AgNPs that contribute to the SPRB (mainly non-aggregated AgNPs) in solution. Therefore, we hypothesised that the oxidation occurred after the aggregation and later sedimentation of the AgNPs. Therefore, confirmation of the oxidation process (see SI) from plotting the ln (dA/dt) vs ln (A) could not be obtained (Videos S7–S8). Even though, the slopes were closer (between 0.30 and 0.50) to the theoretical value of 0.67.

The distinct behaviour of AgNP-GAH was also observed upon introduction to natural fjord waters. In contrast to the other polymers-coated NPs, the complex organic matter content of these waters did not facilitate their stabilization (Figs. 5b and S7d). A two fold reduction in *A* was observed after ca. 40 and 150 min upon addition of AgNP-GAH to 153 and 537 mM NaCl solutions at pH 8, respectively. Nevertheless, when identical NPs were introduced to the natural fjord waters, *A* was reduced by ca. 50% within 15 min. Therefore, a much faster aggregation occurred. This fact was also attributed to the high amount of silver-chloride charged species immediately surrounding the NPs, that interact with the organic matter present in solution and reducing the additional steric-electrostatic stabilization.

4. Conclusions

UV-Visible measurements provided important information on kinetic processes of AgNPs aggregation. UV-Visible spectrophotometry allowed us to obtain unique and valuable information during the first seconds of the AgNP aggregation process, which provided evidence on the first stages of the AgNP aggregation process, of new NP formation from silver ions. Moreover, it also allowed us to distinguish between different stages of the kinetic aggregation process that corresponded to different aggregation rates. The decrease in the *SPRB area* (*A*) also provided confirmation of aggregation as the dominant mechanism, while the analysis of the $W_{h/2}$ provided a good assessment of CCC values. A relatively high AgNP concentration (μM) was used in this study due to the detection limits of the spectrophotometric technique used. As a consequence, the extrapolation of the obtained results to realistic environmental concentrations of AgNPs is not straightforward. The aggregation and dissolution of NPs is influenced by their concentration in solution. Therefore, differences in the aggregation/dissolution rates are expected upon realistic and lower AgNPs discharges in the environment.

Alginate coating showed moderate electrostatic stabilization with a CCC of around 82 mM in NaCl solutions at pH = 8.0. Gum Arabic coating provided AgNP with steric stabilization at low silver ion/silver species concentrations. In contrast, low electrostatic stabilization was obtained with a CCC value of around 41 mM in NaCl solutions containing <60% of silver as AgNPs probably because of changes in the coating layer structure and/or adsorption due to interactions with different silver-chloride species present in excess interacting with the AgNPs. Oxidation only played a significant role for AgNP-GAH as a consequence of the instability of the aggregates, which are oxidised in presence of high concentrations of Ag^+ species. The introduction of ALG and GAL-coated NPs to natural fjord waters indicated a strong stabilization against the aggregation of the NPs by natural organic matter, evidencing the influence of the complex environment in the fjord waters compared to the synthetic NaCl solutions. Terrestrial fulvic/humic-like compounds, observed in the natural fjord waters, are likely responsible for the enhanced stabilization in terms of aggregation rate. Much faster aggregation kinetics were observed for AgNP-GAH in natural fjord waters compared to synthetic NaCl solutions. This was attributed to the high amount of charged silver-chloride species present in solution. Moreover, the effect over aggregation/oxidation kinetics of multivalent ions, e.g. calcium, present in the fjord waters should be also considered. Divalent ions have a greater influence than the monovalent ions in screening and neutralizing the surface charge of NPs. Even if calcium is present in much smaller quantities than sodium (around 50 fold) in seawaters, it presents a higher electrostatic accumulation and a greater affinity for the coating binding sites. For example, the cross-linking reaction that takes place between calcium and the alginate molecules results in a cooperative association of long regions of polymer chains, generating gel-like structures that may reduce the stability of the AgNPs present in the fjord waters due to the modification of the coating structure. This effect, if present, was not as strong as the stabilization against aggregation produced by the organic matter observed in this work.

The type of coating layer has been revealed as a key factor in the aggregation/oxidation behaviour of AgNP in solution. As a consequence, AgNPs behaving like AgNP-ALG or AgNP-GAH readily aggregate in waters with salinities higher than 4.5–9, and their likely fate is sedimentation and kinetic deposition if no additional stabilization from organic matter is considered. In contrast, the behaviour of steric-stabilized AgNPs allows them to remain as non-aggregated NPs for a longer duration in solution, even at salinities of seawater (~35), and consequently they are available for uptake by pelagic marine organism. Therefore, the behaviour of the steric-stabilized AgNPs is much less affected by ionic strength changes than the electrostatic-stabilized AgNPs.

Nevertheless, the ionic strength is not the only factor that influenced the aggregation rate of the polymer-coated AgNPs. The introduction of AgNPs into fjord waters resulted in additional stabilization from organic matter independently of the steric/electrostatic behaviour provided by the polymer coating. The presence of different organic compounds in natural fjord waters appears to modify the expected aggregation behaviour of polymer-coated AgNPs, based on the contribution of NaCl at an equivalent ionic strength. Therefore, even if AgNP coated with alginate and gum Arabic could be considered as appropriate models to simulate the aggregation behaviour of AgNPs, the extrapolation of the results obtained in studies using NaCl solutions to more complex matrices containing organic compounds is not straightforward.

Summary of the synthesis of AgNPs, details about experimental techniques and equipment, AgNPs characterization and natural fjord water characterization. Tables S1–S3, Figs. S1–S8 and Videos S1–S8.

Supplementary data to this article can be found online at http://dx.doi.org/10.1016/j.scitotenv.2015.08.115.

Acknowledgements

This research was supported by a Marie Curie Intra European Fellowship within the 7th European Community Framework Programme (grant agreement number PIEF-GA-2012-329575). Prof. J. Puy, Dr. Calin David and Dr. C. Rey-Castro from the Chemistry Department of Lleida University (Spain) are gratefully acknowledged for their help with the F-FFF measurements and data analysis. King Abdulaziz University is acknowledged for their support.

References

Abe, T., Kobayashi, S., Kobayashi, M., 2011. Aggregation of colloidal silica particles in the presence of fulvic acid, humic acid, or alginate: Effects of ionic composition. Colloids Surf. A 379 (1–3), 21–26.
Amendola, V., Bakr, O., Stellacci, F., 2010. A study of the surface plasmon resonance of silver nanoparticles by the discrete dipole approximation method: effect of shape, size, structure, and assembly. Plasmonics 5 (1), 85–97.
Auffan, M., Bottero, J.Y., Chaneac, C., Rose, J., 2010. Inorganic manufactured nanoparticles: how their physicochemical properties influence their biological effects in aqueous environments. Nanomedicine UK 5 (6), 999–1007.
Baalousha, M., Nur, Y., Römer, I., Tejamaya, M., Lead, J.R., 2013. Effect of monovalent and divalent cations, anions and fulvic acid on aggregation of citrate-coated silver nanoparticles. Sci. Total Environ. 454–455 (0), 119–131.
Baalousha, M., Croteau, M.N., Dawson, K., Goldberg, E.S., How, W., Khan, F.r., Lead, J., Louie, S.M., Lowry, G.V., Luoma, S.N., Lynch, I., Ma, R., Praetorious, A., Scheringer, M., Schirmer, K., Valsami-Jones, E., 2014. Nanoscience and the Environment. 1st ed. Elsevier.
Barriada, J.L., Tappin, A.D., Evans, H.E., Achterberg, E.P., 2007. Dissolved silver measurements in seawater. TrAC Trends Anal. Chem. 26 (8), 809–817.
Benn, T.M., Westerhoff, P., 2008. Nanoparticle silver released into water from commercially available sock fabrics. Environ. Sci. Technol. 42, 4133–4139.
Blaser, S.A., Scheringer, M., MacLeod, M., Hungerbühler, K., 2008. Estimation of cumulative aquatic exposure and risk due to silver: contribution of nano-functionalized plastics and textiles. Sci. Total Environ. 390, 396–409.
Chandrasekhar, S., 1943. Stochastic problems in physics and astronomy. Rev. Mod. Phys. 15 (1), 1–89.
Chappell, M.A., Miller, L.F., George, A.J., Pettway, B.A., Price, C.L., Porter, B.E., Bednar, A.J., Seiter, J.M., Kennedy, A.J., Steevens, J.A., 2011. Simultaneous dispersion–dissolution behavior of concentrated silver nanoparticle suspensions in the presence of model organic solutes. Chemosphere 84 (8), 1108–1116.
Chernousova, S., Epple, M., 2013. Silver as antibacterial agent: ion, nanoparticle, and metal. Angew. Chem. Int. Ed. 52 (6), 1636–1653.
Coble, P.G., 2007. Marine optical biogeochemistry: the chemistry of ocean color. Chem. Rev. 107 (2), 402–418.
Dauqan, E., Abdullah, A., 2013. Utilization of gum Arabic for industries and human health. Am. J. Appl. Sci. 10 (10), 1270–1279.
Derjaguin, B.V., Landau, L., 1941. Theory of the stability of strongly charged lyophobic sols and of the adhesion of strongly charged particles in solutions of electrolytes. Acta Phys. Chim. URSS 14, 633–662.
Espinoza, M.G., Hinks, M.L., Mendoza, A.M., Pullman, D.P., Peterson, K.I., 2012. Kinetics of halide-induced decomposition and aggregation of silver nanoparticles. J. Phys. Chem. C 116 (14), 8305–8313.
Evanoff, D.D., Chumanov, G., 2005. Synthesis and optical properties of silver nanoparticles and arrays. ChemPhysChem 6 (7), 1221–1231.
Fabrega, J., Luoma, S.N., Tyler, C.R., Galloway, T.S., Lead, J.R., 2011. Silver nanoparticles: behaviour and effects in the aquatic environment. Environ. Int. 37 (2), 517–531.
Gallego-Urrea, J.A., Perez Holmberg, J., Hassellov, M., 2014. Influence of different types of natural organic matter on titania nanoparticle stability: effects of counter ion concentration and pH. Environ. Sci.: Nano 1 (2), 181–189.
Gondikas, A.P., Morris, A., Reinsch, B.C., Marinakos, S.M., Lowry, G.V., Hsu-Kim, H., 2012. Cysteine-induced modifications of zero-valent silver nanomaterials: implications for particle surface chemistry, aggregation, dissolution, and silver speciation. Environ. Sci. Technol. 46 (13), 7037–7045.
Haug, A., 1961. Dissociation of alginic acid. Acta Chem. Scand. 15 (4), 950–952.
Huynh, K.A., Chen, K.L., 2011. Aggregation kinetics of citrate and polyvinylpyrrolidone coated silver nanoparticles in monovalent and divalent electrolyte solutions. Environ. Sci. Technol. 45 (13), 5564–5571.
Ishii, S.K.L., Boyer, T.H., 2012. Behavior of reoccurring PARAFAC components in fluorescent dissolved organic matter in natural and engineered systems: a critical review. Environ. Sci. Technol. 46 (4), 2006–2017.
Jayme, M.L., Dunstan, D.E., Gee, M.L., 1999. Zeta potentials of gum Arabic stabilised oil in water emulsions. Food Hydrocoll. 13 (6), 459–465.
Kim, J.S., Kuk, E., Yu, K.N., Kim, J.-H., Park, S.J., Lee, H.J., Kim, S.H., Park, Y.K., Park, Y.H., Hwang, C.-Y., Kim, Y.-K., Lee, Y.-S., Jeong, D.H., Cho, M.-H., 2007. Antimicrobial effects of silver nanoparticles. Nanomed. Nanotechnol. Biol. Med. 3 (1), 95–101.
Lapresta-Fernandez, A., Fernandez, A., Blasco, J., 2012. Nanoecotoxicity effects of engineered silver and gold nanoparticles in aquatic organisms. TrAC Trends Anal. Chem. 32, 40–59.
Levard, C., Hotze, E.M., Lowry, G.V., Brown, G.E., 2012. Environmental transformations of silver nanoparticles: impact on stability and toxicity. Environ. Sci. Technol. 46, 6900–6914.
Li, K., Zhang, W., Huang, Y., Chen, Y., 2011. Aggregation kinetics of CeO2 nanoparticles in KCl and CaCl2 solutions: measurements and modeling. J. Nanopart. Res. 13 (12), 6483–6491.
Lin, S., Cheng, Y., Liu, J., Wiesner, M.R., 2012. Polymeric coatings on silver nanoparticles hinder autoaggregation but enhance attachment to uncoated surfaces. Langmuir 28 (9), 4178–4186.
Ma, R., Levard, C., Marinakos, S.M., Cheng, Y., Liu, J., Michel, F.M., Brown, G.E., Lowry, G.V., 2012. Size-controlled dissolution of organic-coated silver nanoparticles. Environ. Sci. Technol. 46 (2), 752–759.
Moskovits, M., Vlčková, B., 2005. Adsorbate-induced silver nanoparticle aggregation kinetics. J. Phys. Chem. B 109 (31), 14755–14758.
Percival, E., McDowell, R.H., 1967. Chemistry and Enzymology of Marine Algal Polysaccharides. Academic Press, London New York.
Quik, J.T.K., Velzeboer, I., Wouterse, M., Koelmans, A.A., van de Meent, D., 2014. Heteroaggregation and sedimentation rates for nanomaterials in natural waters. Water Res. 48, 269–279.
Rey-Castro, C., Herrero, R., Sastre de Vicente, M.E., 2004. Gibbs–Donnan and specific ion interaction theory descriptions of the effect of ionic strength on proton dissociation of alginic acid. J. Electroanal. Chem. 564, 223–230.
Rizzello, L., Pompa, P.P., 2014. Nanosilver-based antibacterial drugs and devices: mechanisms, methodological drawbacks, and guidelines. Chem. Soc. Rev. 43 (5), 1501–1518.
Sandip, S., Anjali, P., Subrata, K., Suomen, B., Tarasankar, P., 2010. Photochemical green synthesis of calcium-alginate-stabilized Ag and Au nanoparticles and their catalytic application to 4-nitrophenol reduction. Langmuir 26 (4), 2885–2893.
Sharma, V.K., Siskova, K.M., Zboril, R., Gardea-Torresdey, J.L., 2014. Organic-coated silver nanoparticles in biological and environmental conditions: fate, stability and toxicity. Adv. Colloid Interface Sci. 204, 15–34.
Sulzberger, B., Durisch-Kaiser, E., 2009. Chemical characterization of dissolved organic matter (DOM): a prerequisite for understanding UV-induced changes of DOM absorption properties and bioavailability. Aquat. Sci. 71 (2), 104–126.
Thio, B.J.R., Montes, M.O., Mahmoud, M.A., Lee, D.-W., Zhou, D., Keller, A.A., 2011. Mobility of capped silver nanoparticles under environmentally relevant conditions. Environ. Sci. Technol. 46 (13), 6985–6991.
Verwey, E., Overbeek, J., van Nes, K., 1948. The Theory of the Stability of Lyophobic Colloids: The interaction of Sol Particles Having an Electric Double Layer. Elsevier, Amsterdam.